

An Improved Ant Colony System for Retinal Blood Vessel Segmentation

Ahmed Hamza Asad^{1,*}, Ahmad Taher Azar^{2,*}, Mohamed Mostafa M. Fouad^{3,*}
Aboul Ella Hassanien^{4,*}

¹Department of Computer Sciences and Information, ISSR, Cairo University, Egypt

²Faculty of Computers and Information, Benha University, Egypt

³Arab Academy for Science, Technology, and Maritime Transport, Cairo, Egypt

⁴Faculty of Computers and Information, Cairo University, Egypt

*Scientific Research Group in Egypt (SRGE)

<http://www.egyptscience.net>

Abstract—The diabetic retinopathy disease spreads diabetes on the retina vessels thus they lose blood supply that causes blindness in short time, so early detection of diabetes prevents blindness in more than 50% of cases. The early detection can be achieved by automatic segmentation of retinal blood vessels in retinal images which is two-class classification problem. This paper proposes two improvements in previous approach uses ant colony system for automatic segmentation of retinal blood vessels. The first improvement is done by adding new discriminant feature to the features pool used in classification. The second improvement is done by applying new heuristic function based on probability theory in the ant colony system instead of the old that based on Euclidean distance used before. The results of improvements are promising when applying the improved approach on STARE database of retinal images.

I. INTRODUCTION

THE DIABETIC retinopathy is the most common cause of blindness worldwide since the blindness occurs as a result of retina death due to loss of blood supply by the widely spread diabetes on it [1]. The blindness brings significant costs both to individual and society. There are two types of diabetic retinopathy; the first type is the non-proliferative diabetic retinopathy where the capillaries of retina swell and interfere with normal vision. The second type is the proliferative diabetic retinopathy where the capillaries of retina shut down. In both types, the diabetic retinopathy usually leads to retina revascularization [2]. So the segmentation of blood vessels in retinal images is an important step in treatment of diabetic retinopathy. Also there are many other diseases are often diagnosed based on their changes on reflectivity, bifurcations and tortuosity of retinal blood vessels such as hypertension [3]. Retinal blood vessels segmentation is also the core stage in automated registration of two retinal blood vessels images of a certain patient to follow and diagnose his disease progress at different times [4]. The retinal blood vessels segmentation is a classification problem where each pixel in the field of view of retinal image is classified as vessel-like or non-vessel. The manual segmentation of retinal blood vessels is a long and tedious task which also requires training and skill. So, for the last two decades, the automated retinal blood vessels

segmentation attracts a lot of research in the medical image processing area since it's the critical component of circulatory blood vessel analysis systems [5]. The Reliable automated retinal vessel extraction encounters several challenges [6]: “(1) The blood vessels have a wide range of widths from very large (15 pixels) to very small (3 pixels) and diffident bifurcations. (2) Various structures appear in retinal image, including the optic disc, fovea, exudates and pigment epithelium changes, which severely disrupt the automatic vessel extraction. (3) The narrow vessels with various local surroundings may appear as some elongated and disjoint spots, which are usually lost. (4) The vessels intensity contrast is weak and variant and the small vessels especially are overwhelmed by Gaussian-like noises”.

This paper proposes two improvements of the previous approach [7] used for automatic segmentation of blood vessels in retinal images based on the ant colony system (ACS) [8]. The improvements are performed in two ways, first adding new discriminant feature to the features pool to be consisted of fifteen features and second applying new heuristic function in ACS. The features pool consists of features that are simple, fast in computation, needn't to be computed at multiple scales or orientations and highly discriminate between vessels and background in retinal images [9]. These features are based on gray-level of the green image of retina, gray-level of computed vessels-enhanced image and Hu moment-invariants [10]. Since the large number of computed features increases the classification complexity, time and reduces its accuracy, so feature selection is an essential step for successful classification because it removes irrelevant features and achieves less complex, more accurate and faster classification. In this paper, the correlation based feature selection heuristic (CFS) [11] is used and it reduced the features set from fifteen to the best four features set. The performance of this improved approach is evaluated on a publicly available STARE database of retinal images [12] for scientific research in terms of the sensitivity, specificity and accuracy. Thus it's the first paper that tests ACS performance on STARE database. The rest of this paper is organized as follows: Section II surveys the previous popular related work. Section III presents scientific background on

the used features, CFS and ACS. Section IV presents the proposed approach and its improvements. In section V, there are experimental results. Finally in Section VI, conclusions and directions for future research are presented.

II. RELATED WORK

The automatic segmentation methods of retinal blood vessels are categorized into supervised and unsupervised. In this section, short survey of popular retinal blood vessels segmentation methods from two categories is presented. This short survey shows how these methods were developed in the last two decades. For the supervised methods, they depend on pixel classification into vessel class or non vessel class using a classifier previously trained on manually-labelled samples by ophthalmologists from two classes. So these methods depend on pre-classified data which mayn't be available in real life applications. Also there are significant differences between ophthalmologists themselves in delineation of blood vessels. The training makes these methods give better performance than unsupervised methods especially in healthy images. Staal et al. [13] used KNN-classifier with 27-D feature vector based on ridges information. Their method depends on extracting ridges in the image, forming line elements from ridges, assigning each pixel to nearest line to partition image into patches and computing features vector of each pixel based on its line and patch attributes. Then the feature vector reduced to those result in best class separability by sequential forward selection algorithm. Ricci and Pefetti [14] used 3-D feature vector consists of the inverted gray-level of green color plus the two maximum responses of two orthogonal line detectors rotated in twelve angles and their classifier was the support vector machine (SVM). Marin et al. [9] used 7-D feature vector consists of five features encode gray-level variation between pixel and its surroundings plus other two features based on Hu moment-invariants and their classifier was the neural network (NN). Fraz et al. [15] used 9-D feature vector consists of the inverted gray-level of green color, the sum of gradient orientation maps at three scales, sum of tophat transform responses in eight directions using linear structure element, the two maximum responses of two orthogonal line detectors rotated in twelve angles and the four maximum responses of Gabor filter rotated in ten angles at four scales. They used an ensemble classifier from two-hundred bagged and boosted decision trees.

For the unsupervised methods, they are classified into methods based on mathematical morphology, vessel tracking, matched filter, bio-inspired algorithms and active contour. For the methods based on mathematical morphology, they utilize the fact that retinal vessels have morphology of connected piecewise linear segments. The top-hat morphological transformation is widely used in blood vessels segmentation since it estimates the background of retinal image using morphological opening operation and the retinal vessels are better enhanced when subtracting this estimated background from original image. The advantages of mathematical morphology are the speed and noise resistance but its drawback is that it doesn't

exploit the known shape of retinal vessel cross-section. Miri and Mahloojifar [16] used the fast discrete Curvelet transform (FDCT) for contrast enhancement and multi-structure morphological transformation for detection of retinal vessels edges. The false positive detections are pruned by morphological opening by reconstruction and length filtering. Fraz et al. [17] extracted the centerlines of retinal vessels using first-order derivative of Gaussian (FODOG) filter rotated in four orientations to detect retinal vessels in all directions. Then the shape and orientation maps of the retinal vessels are produced by applying morphological top-hat transform with linear structuring element at eight directions to emphasis vessels in all possible orientations followed by morphological bit plane slicing of gray-level image. The final vessels tree is reconstructed using detected centrelines and maps of shape and orientation.

For the methods based on vessel tracking, they work at single retinal vessel rather than entire retinal vasculature. Starting with initial set of pixels as seeds that are selected automatically or manually labelled, the trace of a vessel is done based on pixels local information by selecting the next candidate pixel in the retinal vessel from set of pixels that are closed to current pixel under consideration. The main advantage of these methods is providing information about single vessel such as its width, connectivity and branching. Their drawback is the need for good initial set of pixels to trace all retinal vessels or they may be missed especially at bifurcations and crossings. Kelvin et al. [18] initially determine sparse seed points along the vessel boundary and found the optimal contours connecting these points using Dijkstras algorithm. After that, they used cost function incorporates Frangis multiscale vesselness measure, vessel direction consistency, the edge evidence and the spatial and radius smoothness constraints into conventional Livewire framework to efficiently compute optimal vessels medial axes. Delibasis et al. [19] initialized the seeds pixels for vessel tracking using a multiscale vesselness filter and picked a random non-zero pixel as a seed. They utilize a parametric model that exploits the geometric properties of retinal vessel composed of a "stripe" and they defined a measure of match (MoM) which quantifies the similarity between the model and the given image. The vessel tracking is done by identifying the best matching strip with the vessel by using the seed point, strip orientation, strip width and the MoM. This method actively seeks vessel bifurcation, without user intervention.

For the methods based on matched filter, the matched filter is 2-D kernel convolved with the image to search for three features of retinal vessel in the image at unknown position and orientation. These features should be considered when designing a matched filter; (1) intensity profile of cross-section of a retinal vessel is approximated by Gaussian curve so the matched filter has Gaussian profile. (2) The retinal vessel has little curvature so it can be approximated by piecewise linear segments. (3) The retinal vessel diameter decrease as it moves outward from the optic disk. The kernel is rotated in multiple orientations to detect the all vessels in all directions so it takes more computation overhead. The response of matched filter is

high with retinal vessels that have the same standard deviation of Gaussian function modelled by matched filter so it may miss retinal vessels that have different profiles. The illumination variation in background and presence of pathologies increases false positive detections resulted by the matched filter. Al-Rawi et al. [20] applied exhaustive search based optimization on DRIVE retinal images database [13] to find optimal values of matched filter parameters such as size, standard deviation and threshold. Zhang et al [21] extended the matched filter by using two kernels; one based on Gaussian and another based on first derivative of Gaussian (FODOG) to filter out false positive detections resulted by matched filter such as non vessel edges which has high responses to both kernels while vessels has high responses only to the basic Gaussian-profiled matched filter.

For the methods based on bio-inspired algorithms, little work was done used ACS. Cinsdikici and Aydn [22] fused the results of ACS and matched filter using OR operator to construct the final segmentation result. Hooshyar and Khayati [23] used fuzzy ACS where the maximum eigenvalue of Hessian matrix at multiples scales and the maximum response of Gabor filter at multiple orientations are the features of each pixel. Asad et al. [7] used ACS standalone where the features of each pixel are simple because they are based on gray-level variations between it and its surroundings in green color of retinal image and the known Hu moment-invariants. These features don't need to be computed at multiple scales or orientations, so they are fast on computation.

For methods based on active contour, the active contour (snake) is initialized curve moves on the image under internal forces by the curve itself and external forces by the image data. Both types of forces are defined so that the snake fits to a desired feature in the image. The external forces are defined by a human user or supervising process. The active contour are used in edge detection, shape recognition and object tracking. The advantage of active contour for example in shape recognition is that it's independent and self-adapting so it conforms to any shape but its drawback is that it needs to be initialized close to the search target to avoid local minima. Espona et al. [24] initially mapped vessel creases using the multilevel set extrinsic curvature based on structure tensor. Next tracing of the optic nerve circumference is performed to initialize an active contour at the intersection of vessel creases with this circumference. The active contour is deformed influenced by external forces of vessel creases. Al-Diri et al. [25] initially used tramline filter to segment some pixels of likely vessel centerline then the segment growing algorithm initialized multiple vessels segments from these segmented pixels using pairs of active contours. The twins active contours conformed to vessels edges while the bifurcations and crossings are extended using the junction resolution algorithm.

III. BACKGROUND

A. Features

The features pool consists of the gray-level of green channel of RGB retinal image (*green*), group of five features based on the green gray-level ($f1, f2, f3, f4, f5$), group of eight features based on Hu moment-invariants ($Hu1, Hu2, Hu3, Hu4, Hu5, Hu6, Hu7, Hu8$) and the gray-level of the vessels-enhanced image (*Ive*) [7]. Most of the vessels segmentation approaches extract and use the green color image of RGB retinal image for further processing since it has the best contrast between vessels and background so it's taken as feature. The five gray-level based features group is presented by Marin et al. [9] and its features describe the gray-level variation between vessel pixel and its surrounding. The Hu moment-invariants are best shape descriptors which are invariant to translation, scale and rotation change. So they are used by the second group of eight features to describe vessels have variant widths and angles. The vessels-enhanced image [9] is better enhancing blood vessels while removing the bright retinal structures as optic disc and exudates, so it's used for computing the group of eight Hu moment invariants based features and its gray-level (*Ive*) is the new added feature to the previous features pool as first improvement. These features are simple, better discriminate between vessel and non-vessel classes and needn't be computed at multiple scales or orientations. The features computation is more detailed in [7].

B. Correlation Based Feature Selection Heuristic

It's a heuristic approach for evaluating the worth or merit of a subset of features [11]. The main premise behind this selection method is that the features that are most effective for classification are those that are most highly correlated with the classes (intensifiers and dissipaters), and at the same time are least correlated with other features. The method is therefore used to choose a subset of features that best represent these qualities. The best individual feature based on the following merit metric:

$$M_s = \frac{kr_{cf}}{\sqrt{k+k(k-1)r_{ff}}} \quad (1)$$

where M_s is the heuristic merit of a features subset S containing k features, r_{cf} and r_{ff} are the average feature-class correlation and the average feature-feature inter-correlation respectively. The numerator gives an indication of how predictive a group of features are; the denominator of how much redundancy there's among them.

C. Ant Colony System

The ACS as meta-heuristic searching algorithm was first proposed by Dorigo et al. [8] for solving the travelling sales man problem (TSP). The ACS is based on simulating the foraging behaviour of real ants in nature. In nature when real ants are searching for foods, multiple ants are going out in random paths. As the ant is moving, it deposits a chemical substance which is called pheromone on its moving path for guiding other subsequent ants to its path. As the time goes,

the pheromone is evaporating. So as the path is shorter as its pheromone concentration remains more time and more other ants are attracted to it. Thus the shortest path is the only one which attracts other ants. ACS is more detailed in [7].

IV. PROPOSED APPROACH

After features selection process by CFS heuristic and determining its recommended features set for STARE databases ($f2, f5, Hu1, Ive$), the proposed approach is applied to retinal images. It consists of four phases; preprocessing, features computation, ACS based segmentation and post-processing. In preprocessing phase, the green channel of RGB retinal image is extracted and its contrast is better enhanced by covering the whole range of intensity [0, 255] since it's a feature($green$) and it's used in further processing. After that, the central light reflex which runs down the central length of some vessels is removed. In features computation phase, the varying illumination in background is corrected by computing the homogenized background image for better discriminating vessels from background and computing the gray-level based features ($f2, f5$). Finally, the vessels-enhanced image is computed since its gray-level (Ive) is used for computing Hu moment-invariants based feature ($Hu1$) as well as it's selected feature by CFS. In The ACS based segmentation phase, each pixel is classified as vessel or background depending on its pheromone level τ and heuristic function η value. The old heuristic function η was the Euclidean distance between the target pixel and both centers of vessels and background classes in the feature space:

$$\eta = \frac{\text{Euclidean distance to background class center}}{\text{Euclidean distance to vessels class center}} \quad (2)$$

The class center consists of averages of all selected features by CFS over all training pixels of the database. From the final pheromone map image τ , the vessels are segmented from background by thresholding. In post processing phase, linking of disjoint pixels is performed by setting pixel to 1 if it's surrounded at least by four neighbouring pixels of 1; otherwise it's set to 0. All small regions have area less than 20 are filtered out. Finally, a median filter of size 3*3 eliminates all remaining isolated noisy pixels. Algorithm (I) shows the proposed approach which is more detailed in [7].

As second improvement, new heuristic function based on probability theory is applied to enhance the performance of proposed approach. The heuristic function is also computed from all training pixels of the database. So for probability calculation, the values of features in the feature space are transformed to specific interval and rounded to the nearest integers inside this interval. The following equation defines the new heuristic function η^* :

$$\eta^* = \frac{P(v/Vessels)}{P(v/Background)} \quad (3)$$

where $P(v/Vessels)$ and $P(v/Background)$ are the likelihood of feature value v for vessels and background classes respectively.

Algorithm 1 PROPOSED APPROACH

```

1: /* Preprocessing Phase*/
2: Extraction of the green channel of retinal image
3: Linear transformation of its intensity to cover the whole intensity
   range [0, 255]
4: Remove of the central light reflex from it.
5: Computation of its homogenized-background image.
6: Computation of its vessels-enhanced image.
7: /* Features Computation Phase*/
8: for each pixel in the homogenized-background image do
9:   Compute its gray-level based features ( $f2, f5$ )
10: end for
11: for each pixel in the vessels-enhanced image do
12:   Compute its Hu moment-invariants based feature ( $Hu1$ )
13: end for
14: /* ACS based segmentation */
15: Initialize ACS parameters and the pheromone map image
16: Compute the heuristic function based on Eq.3 for each pixel in
   the image
17: Apply ACS operation
18: Threshold the resulted ACS pheromone map image to segment
   vessels from background
19: /* Post-processing */
20: for each pixel in the thresholded image do
21:   if surrounded by at least four neighboring pixels of 1 then
22:     Setting it to 1
23:   else
24:     Setting it to 0
25:   end if
26: end for
27: for each region in the thresholded image do
28:   if area is less than 20 then
29:     Removing it by morphological opening using disk structure
     element
30:   end if
31: end for
32: Applying median filter of size 3*3 to remove all remaining
   isolated pixels

```

V. EXPERIMENTAL RESULTS

A. Material

The STARE database, originally collected by Hoover et al. [12], comprises 20 eye fundus color images (ten of them contain pathology) captured with a TopCon TRV-50 fundus camera at 35 degree field of view (FOV). The images were digitalized to 700*605 pixels, 8 bits per color channel and are available in PPM format. The database contains two sets of manual segmentations made by two different observers. The FOV binary mask for each image isn't available, so we create it by hand for each image using MATLAB function named "impoly" which creates an interactive draggable and resizable polygon on the image to specify the FOV. Also the images aren't divided into separated train and test sets, so the training pixels are selected from the manual segmentations made by the first observer. The segmentation performance of the proposed approach is compared against the segmentations of the second observer as ground truth.

B. Samples Selection

The STARE training set contains 919308 vessels pixels and 5281987 non-vessels (background) inside FOV. These pixels

needed to select samples from them for computation of the best features set using CFS heuristic. Since the ratio of vessel pixels to background pixels in each image and overall images is 1:9 on average, the samples set consists of randomly selected 1000 vessels pixels and 9000 background pixels from each image; there are 20 images give 200000 total samples. The best features set consists of the most repeated features resulted from multiple runs of CFS.

C. Results

Three measures are calculated for evaluating the segmentation performance of recommended features set by CFS with ACS. The first measure is the sensitivity (SN) which is the ratio of well-classified vessels pixels. The second measure is the specificity (SP) which is the ratio of well-classified background pixels. The third measure is the accuracy (ACC) which is the ratio of well-classified vessel and background pixels. Tables I and II show the ACS performance values with the old η and new heuristic function η^* respectively. It's shown from both tables that new heuristic function η^* improves largely the average performance of the ACS especially in sensitivity which increased by about 10% while specificity increased by 1% and accuracy increased by 2%. In the normal images set, the least performance of ACS with the old heuristic function was on image 7 but it's improved when using the new heuristic function; in sensitivity from 0.6608 to 0.9289, in specificity from 0.9005 to 0.9269 and in accuracy from 0.8742 to 0.9271. Also in the abnormal images set the least performance of ACS with the old heuristic function was on image 6 but it's improved when using the new heuristic function; in sensitivity from 0.6472 to 0.8188, in specificity from 0.8883 to 0.9213 and in accuracy from 0.8670 to 0.9122.

TABLE I
PERFORMANCE OF ACS WITH OLD HEURISITC FUNCTION

Image Number	SN	SP	ACC
01	0.6863	0.9565	0.9272
02	0.7210	0.9035	0.8869
03	0.8656	0.8966	0.8941
04	0.7965	0.9043	0.8933
05	0.7453	0.9301	0.9074
06	0.6472	0.8883	0.8670
07	0.6608	0.9005	0.8742
08	0.7493	0.9056	0.8897
09	0.7696	0.9216	0.9053
10	0.6645	0.9012	0.8751
11	0.7329	0.9098	0.8925
12	0.7412	0.9214	0.9024
13	0.7932	0.9271	0.9108
14	0.7680	0.9319	0.9115
15	0.8397	0.9377	0.9262
16	0.8038	0.9358	0.9174
17	0.6472	0.9188	0.8855
18	0.7351	0.8458	0.8381
19	0.8980	0.8865	0.8872
20	0.8316	0.8759	0.8718
Average	0.7549	0.9100	0.8932

Fig.1 and Fig.2 compare between the average performances of ACS with the old η and new heuristic η^* functions with

TABLE II
PERFORMANCE OF ACS WITH NEW HEURISITC FUNCTION

Image Number	SN	SP	ACC
01	0.8071	0.9157	0.9039
02	0.7305	0.9077	0.8915
03	0.8762	0.8921	0.8908
04	0.7684	0.9098	0.8953
05	0.7631	0.9263	0.9063
06	0.8188	0.9213	0.9122
07	0.9289	0.9269	0.9271
08	0.9391	0.9211	0.9229
09	0.9085	0.9385	0.9353
10	0.8368	0.9197	0.9106
11	0.9124	0.9223	0.9213
12	0.9204	0.9384	0.9365
13	0.8700	0.9432	0.9343
14	0.8779	0.9431	0.9350
15	0.8590	0.9371	0.9280
16	0.7824	0.9437	0.9211
17	0.8610	0.9401	0.9304
18	0.8805	0.8912	0.8905
19	0.8831	0.8881	0.8878
20	0.8500	0.9022	0.8974
Average	0.8537	0.9214	0.9139

respect to normal and abnormal images in STARE database. It's shown from Fig.1 that ACS with the new heuristic function outperforms ACS with the old heuristic function with respect to normal images by about 13.5% in sensitivity, 1.5% in specificity and 2.7% in accuracy. Also in Fig.2 the ACS with new heuristic function outperforms the ACS with old heuristic function with respect to abnormal images by about 6% in sensitivity, 1% in specificity and 1.4% in accuracy.

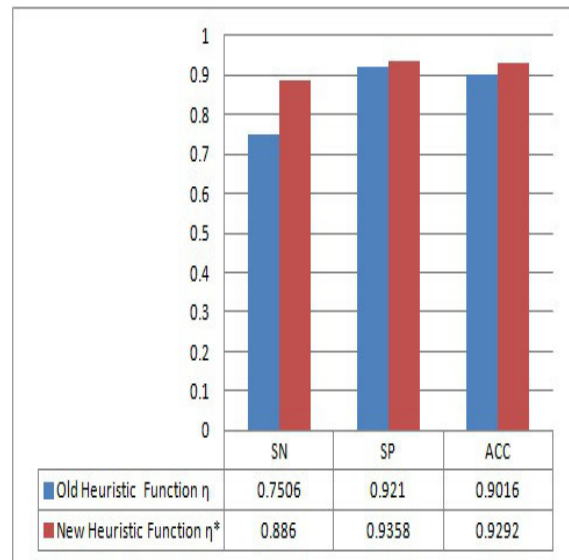


Fig. 1. ACS Performance on Normal Images in STARE

Fig.3 shows how ACS with the new heuristic function outperforms ACS with the old heuristic function in segmenting the small capillaries and bifurcations Fig.3-(d) with fewer false positives Fig.3-(h). So its better to use the new heuristic

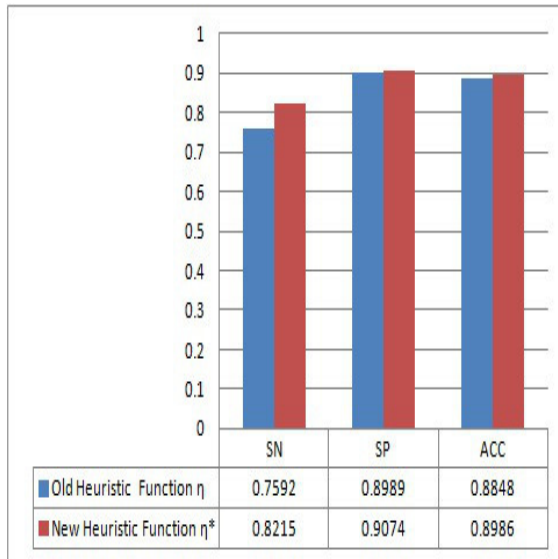


Fig. 2. ACS Performance on Abnormal Images in STARE

function that's based on probability theory instead of the old one that's based on Euclidean distance. Table III shows the performance comparison of the state of art methods as well as the old and improved approaches on SATRE database where the empty cells aren't reported by their authors. Both the old and improved approaches give the best largest sensitivity over the state of art methods. But their values of specificity are the lowest due to high false positives that affected negatively on their accuracies. Although this improved approach gives performance less than performances of state of art methods but its results are promising because they are obtained without learning and using complex features need to be computed at multiple scales and orientations. With respect to the time consumed by this improved approach, for single retinal image the selected four features computation takes on average forty two seconds while the ACS phase takes on average two minutes and forty five seconds on PC with Intel Core-i3 CPU at 2.53 GHz and 3 GB of RAM.

TABLE III
PERFORMANCE COMPARISON OF STATE OF ART METHODS

Method	SN	SP	ACC
Second Human Observer	0.8949	0.9390	0.9354
Staal et al. [13]	0.6970	0.9810	0.9516
Ricci and Pefetti [14]	-	-	0.9646
Marin et al. [9]	0.6944	0.9819	0.9526
Fraz et al. [15]	0.7548	0.9763	0.9534
Hoover et al. [12]	0.6751	0.9567	0.9267
Fraz et al. [17]	0.7311	0.9681	0.9442
Old Approach	0.7549	0.9100	0.8932
Improved Approach	0.8537	0.9214	0.9139

VI. CONCLUSION

The automated extraction of blood vessels in retinal images is an important step in early diagnoses of diabetic retinopathy

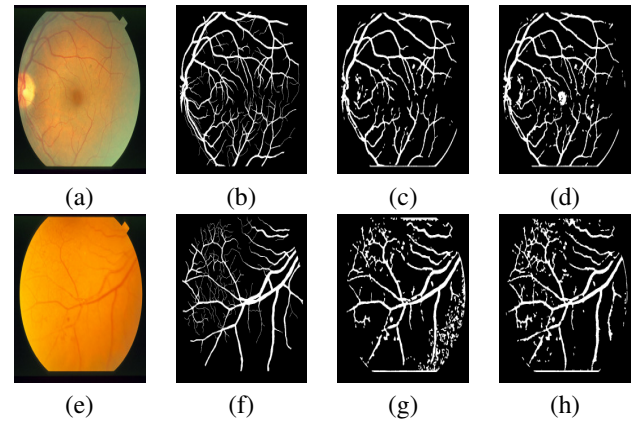


Fig. 3. ACS performance with old and new heuristic functions on normal and abnormal image: (a),(e) retinal image; (b),(f) manual segmentation by second observer; (c),(g) results of ACS with old heuristic function; (d),(h) results of ACS with new heuristic function

and prevention of visual loss since diabetic retinopathy leads to retina revascularization. This paper presents an approach for automatic segmentation of blood vessels in retinal images using ACS based on features that are simple, fast in computation, needn't to be computed at multiple scales or orientations and highly discriminate between vessels and background in retinal images. The paper improves the features by adding new discriminant feature which is selected by CFS heuristic within the best features set. The paper also improves the performance of ACS using new heuristic function based on probability theory instead of the old one which is based on Euclidean distance. The paper is the first one that tested ACS performance on STARE database while the other two papers that also perform ACS-based segmentation of retinal images tested on DRIVE database. The improved approach sensitivity is the largest among the state of art methods. Because of simplicity of its used features, it can be more improved in future to give comparable performance to state of art methods especially by focusing on false positives reduction to increase its specificity and accuracy. Also in future it's needed to assess this improved approach performance on other databases of retinal images such as the DRIVE database.

REFERENCES

- [1] K. Goatman, A. Charnley, L. Webster and S. Nussey, "Assessment of automated disease detection in diabetic retinopathy screening using two-field photography," PLoS. One, vol. 6, no.12, pp. 275-284, 2011.
- [2] K. Verma, P. Deep and A.G. Ramakrishnan, "Detection and classification of diabetic retinopathy using retinal images," Annual IEEE India Conference (INDICON), pp. 1-6, 2011, DOI: 10.1109/INDICON.2011.6139346.
- [3] M. Foracchia, E. Grisan and A. Ruggeri, "Extraction and quantitative description of vessel features in hypertensive retinopathy fundus images," In Book abstracts of 2nd international workshop on computer assisted fundus image analysis, 2011.
- [4] V. Vijayakumari and N. Suriyanarayanan, "Survey on the detection methods of blood vessel in retinal images," Eur. J. Sci. Res., vol. 68, no.1, pp. 83-92, 2012.
- [5] M.M. Fraz, P. Remagnino, A. Hoppe, B. Uyyanonvara, A.R. Rudnicka, C.G. Owen and S.A. Barman, "Blood vessel segmentation

- methodologies in retinal images-a survey," *Comput. Methods Programs Biomed.*, vol. 108, no.1, pp.407-433, October 2012, doi: 10.1016/j.cmpb.2012.03.009.
- [6] X. You, Q. Peng, Y. Yuan, Y. Cheung and J. Lei, "Segmentation of retinal blood vessels using the radial projection and semi-supervised approach," *Pattern Recogn.*, vol. 441, pp. 2314-2324, 2011.
- [7] Ahmed. H. Asad, A. T. Azar, and A. E. Hassanien, "Integrated features based on gray-level and Hu moment invariants with ant colony system for retinal blood vessels segmentation," *Int. J. Syst. Boil. Biomed. Tech.*, vol. 1, no. 4, pp. 61-74, 2012.
- [8] M. Dorigo and L.M. Gambardella, "Ant colony system: a cooperative learning approach to the traveling salesman problem," *IEEE Trans. Evol. Comput.* vol. 1, no. 1, pp. 53-66, 1997.
- [9] D. Marin, A. Aquino, ME. Gegundez-Arias and JM. Bravo, "A new supervised method for blood vessel segmentation in retinal images by using grey-level and moment invariants-based features," *IEEE Trans. Med. Imaging*, vol. 30, no. 1, pp. 146-158, 2011.
- [10] M.K. Hu, "Visual pattern Recognition by Moment Invariants," *IRE. Trans. Inform. Theory.*, vol. 8, no. 2, pp. 179-187, 1962.
- [11] M.A. Hall, "Correlation-based feature felection for discrete and numeric class machine learning," *ICML*, pp. 359-366, 2000.
- [12] A. D. Hoover, V. Kouznetsova, and M. Goldbaum, "Locating blood vessels in retinal images by piecewise threshold probing of a matched filter response," *IEEE Trans. Med. Imaging* , vol. 19, no. 3, pp. 203-210, Mar.2000.
- [13] J.J. Staal, M.D. Abramoff, M. Niemeijer, M.A. Viergever and B. van Ginneken, "Ridge based vessel segmentation in color images of the retina," *IEEE Trans. Med. Imaging*, vol. 23, no. 4, pp. 501-509, 2004.
- [14] E. Ricci and R. Perfetti, "Retinal blood vessel segmentation using line operators and support vector classification," *IEEE Trans. Med. Imaging*, vol. 26, no. 10, pp. 1357-1365, Oct. 2007.
- [15] M. M. Fraz, S. A. Barman, P. Remagnino, A. Hoppe, A.Basit, B. Uyyanonvara, A. R. Rudnicka, and C.G. Owen, "An ensemble classification-based approach applied to retinal blood vessel segmentation," *IEEE Trans. Biomed. Eng.*, vol. 59, no. 9, pp. 1427-1435, Sep. 2012.
- [16] M. S. Miri and A. Mahloojifar, "Retinal image analysis using curvelet transform and multistructure elements morphology by reconstruction," *IEEE Trans. Biomed. Eng.*, vol. 58, no. 5, pp. 1183-1192, May 2011.
- [17] M. M. Fraz, S. A. Barman, P. Remagnino, A. Hoppe, A.Basit, B. Uyyanonvara, A. R. Rudnicka, and C.G. Owen, "An approach to localize the retinal blood vessels using bit planes and centerline detection," *Comput. Methods Programs Biomed.*, Sep. 2011.
- [18] P. Kelvin, H. Ghassan and A. Rafeef, "Live-vessel: extending livewire for simultaneous extraction of optimal medial and boundary paths in vascular images", in *Proc. 10th Int. Conf. Med. Image Computing and Computer-Assisted Intervention*, Springer-Verlag, Brisbane, Australia, 2007.
- [19] K.K. Delibasis, A.I. Kechrinotis, C. Tsonos and N. Assimakis, "Automatic model-based tracing algorithm for vessel segmentation and diameter estimation," *Comput. Method. Programs. Biomed.*, vol. 100, pp. 108-122, 2010.
- [20] M. Al-Rawi, M. Qutaishat, and M. Arrar, "An improved matched filter for blood vessel detection of digital retinal images," *Comput. Biol. Med.*, vol. 37, pp. 262-267, 2007.
- [21] B. Zhang, L. Zhang, L. Zhang and F. Karray, "Retinal vessel extraction by matched filter with first-order derivative of Gaussian," *Comput. Biol. Med.* vol. 40 , pp. 438-445, 2010.
- [22] M.G.Cinsdikici and D.Aydn, "Detection of blood vessels in ophthalmoscope images using MF/ant (matched filter/ant colony) algorithm," *Comput. Methods Programs Biomed.* vol. 96, no. 2, pp. 85-95, 2009.
- [23] S. Hooshyar and R. Khayati, "Retina vessel detection using fuzzy ant colony algorithm," in *Proc Canadian Conf. Computer and Robot Vision (CRV)*, Ottawa, pp. 239-244, 2010.
- [24] L. Espona, M.J. Carreira, M.G. Penedo, M. Ortega, "Retinal vessel tree segmentation using a deformable contour model, in *Proc 19th international Conf. Pattern Recognition (ICPR)*, pp. 1-4, 2008.
- [25] B. Al-Diri, A. Hunter, D. Steel, "An active contour model for segmenting and measuring retinal vessels," *IEEE Trans. Med. Imaging*, vol. 28, pp. 1488-1497, 2009.